**EB2016-SVM-047**

# Updating and design sensitivity processes applied to drum brake squeal analysis

[1,3]Martin, Guillaume[*]; [1,3]Balmes, Etienne; [1]Vermot-Des-Roches, Guillaume ; [2]Chancelier, Thierry
[1]SDTools, France; [2]Chassis Brakes International, France; [3]Arts & Metiers ParisTech, PIMM, France

KEYWORDS – Junction models, Component and assembly modes, Parametric model reduction, Model updating

ABSTRACT – Squeal occurrences are quite common in brakes in production and involve coupling of modes. Detailed understanding of vibration patterns typically requires FEM models updated using test results. The process used at Chassis Brakes International typically starts by updating components so that the main sources of variability are associated with junctions. A modeling strategy allowing the practical analysis of the impact of junctions is proposed and illustrated on the case of a drum brake assembly. As the level of uncertainty/design freedom is fairly large for junctions, the evolution of modal properties is difficult to interpret. The notion of component modes within a rigid assembly is thus introduced and shown to provide an appropriate interpretation of changes in a system with multiple modal crossings. The analysis of possible forced responses is finally shown to lead to relevant interpretation of possibly interesting designs or problematic instances of a variable component.

## INTRODUCTION

Squeal events are quite common on brakes in production, but the final customer wants the highest comfort level in vehicle. To obtain an accurate evaluation of the phenomena, experimental measurements (Experimental Modal Analysis, Operational Deflection Shapes) are useful, but often not sufficient to deeply understand the system behavior or allow the evaluation of potential redesigns. A combination of test and finite element modelling is thus generally involved.

A first objective of tests is to ensure the good test/FE correlation: the model must be accurate enough to be considered as predictive for further analysis. Obtaining sufficient correlation typically implies the use of an updating protocol in a time frame compatible with product development. The protocol used at Chassis Brake International is detailed in section 1.

As component updating reliably leads to predictive models of brake components, the next step is the assembly of multiple components into a system. The only change is thus associated to the modeling of junctions, which are composed of surfaces where contact and sliding can occur. The focus of section 2 is thus choosing a representation of junctions and proposing strategies to analyze their effect on the modal properties of assemblies. The use of in-plane and out-of-plane stiffness is first motivated and shown to lead to major shifts of frequencies with multiple modal crossings. Model reduction is then introduced to reduce computation times and memory requirements. It is validated on the drum brake test case.
Obtaining a clear understanding of modal coupling between different component modes in the presence of variable contact stiffness is difficult so that additional tools are needed. Section 3 thus introduces the idea of computing assembly modes with rigid components. These modes

are shown to be visible in the complete assembly and ease the interpretation of mode crossings.
Finally, going back to squeal occurrences, the difficulty is generally due to modal coupling. As junctions play a major role and can vary between different brakes or for different operating conditions of the same brake, mastering the effect of junctions on modal properties and coupling between different component modes is thus critical. To illustrate the process section 4 analyses the evolution of sampled transfer functions for variable junction properties.

Throughout the paper, developments will be applied to an industrial test case of a partial drum brake assembly combining a plate connected to a cable guide by a block and two rivets (see Figure 1 left). The effect of rivets is to apply a force that maintains contact between the other components but due to imperfectly flat surfaces and limited pressure between stiff parts, the true extent of the contact surface is not perfectly controlled. In the FEM the rivets can be and are ignored since their main contribution is to generate a contact surface [1] and their mass contribution can be incorporated otherwise (see Figure 1 right).

Figure 1 : Experimental setup (left), FEM model(right)

1. COMPONENT MODE CORRELATION AND UPATING

The classical way to build the finite element model is first to take the generated meshes from the CAD of each component. Material parameters are then defined with expected nominal values. Finally, the model is assembled by defining the link between components on their contact surface (often using a fully constrained contact on the whole surface).

In many cases, especially at high frequency, models defined this way are not well correlated with experimental measurements, mainly due to error sources: the geometry, the material properties and the contact definition of junctions. To address these sources, the updating protocol used at Chassis Brakes International is defined in three steps illustrated inFigure 2. Rather than using the CAD geometry, the physical geometry is measured and reconstructed (directly from scratch and meshed or using morphing techniques for the initial FEM to fit the measured point cloud). Once the component geometry is accurate, the component material properties are tuned. Density is updated using physical part weight and Young modulus from paired modal frequencies: identified (through EMA) and numerical ones. This process has proved to reliably provide component models [2].

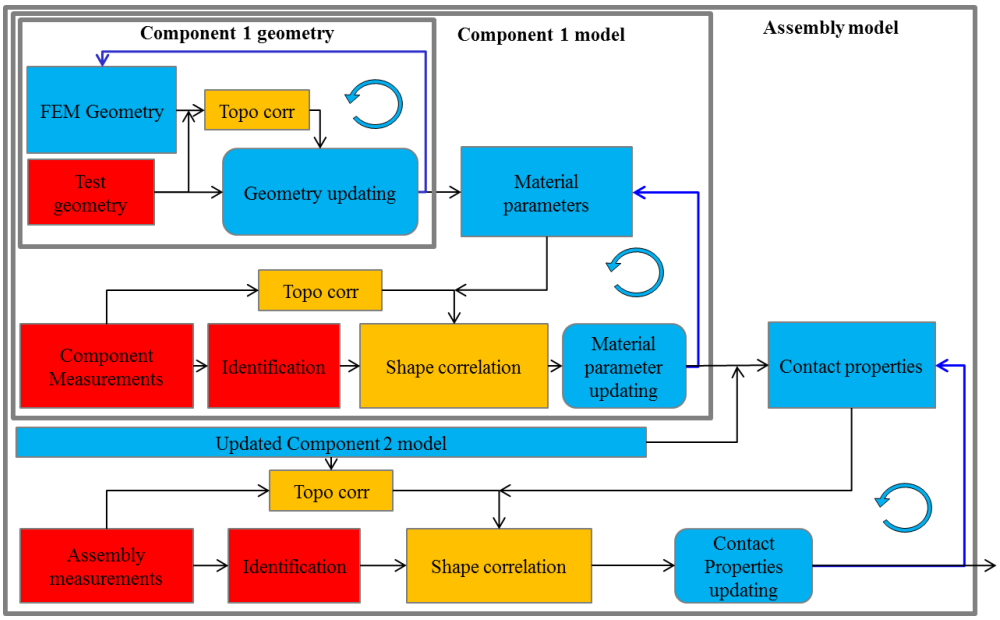

Figure 2 : Updating protocol: component geometry, component properties, contact properties of assemblies.

As an example, the correlation between the test case and the nominal FEM (CAD geometry meshed, nominal material properties and fully constrained contact between components) is shown in Figure 3. Taking the test case presented above, an Experimental Modal Analysis was performed with a 3D laser vibrometer. As illustrated in Figure 3 left, the wireframe corresponding to localization of sensors is first superposed to the FEM. The numerical modeshapes are then observed at the sensor locations to obtain two comparable sets of modeshapes. The correlation is then obtained from the classical Modal Assurance Criterion [3]. Figure 3 right shows a MAC with many mode switches and even some experimental modeshapes that do not have any numerical match. In the present case, the initial correlation is already quite good and updating the components only marginally improves assembly correlation. In [2] the focus is made on a similar drum plate updating and the key role of the geometry is addressed.

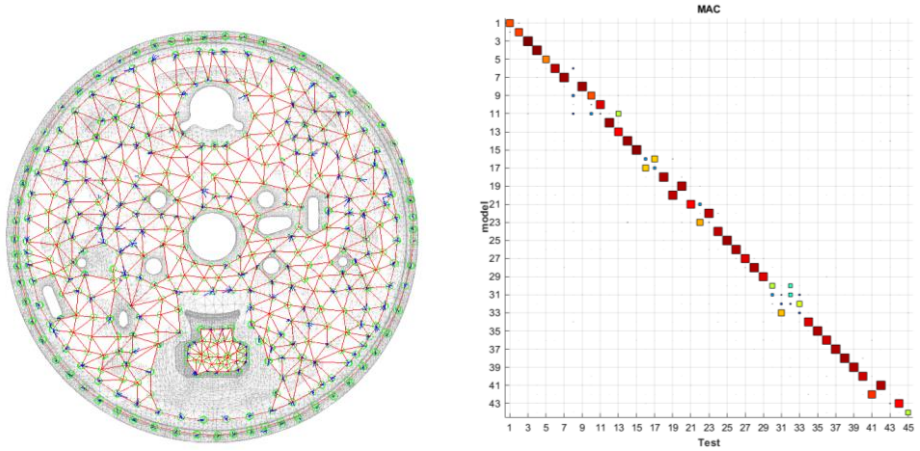

Figure 3 : Test / FEM superposition (left); MAC between numerical and experimental modeshapes (right)

Further testing showed that, at component level, the experimental dispersion between multiple components leads to relative frequency shifts, typically of +/- 2%. Whereas, when measuring several assemblies, some modes exhibit much dispersion up to +/- 10%. The need to analyze junctions is thus clearly established.

## 2. REPRESENTING JUNCTION PROPERTIES AND ANALYSING THEIR EFFECT

A major unknown in most assemblies is the actual surface where the pressure is sufficient to maintain contact with or without sliding. It is known that the assembly is functional so that minimum contact is always maintained, but, in many situations, a notable fraction of the surfaces touching in the nominal CAD model are actually not in contact. Figure 4 illustrates the minimum and maximum surfaces that could be in contact. A node to surface contact is introduced so that the interior nodes close to the rivets are assumed to always be in perfect contact while the status of all others is potentially unknown.

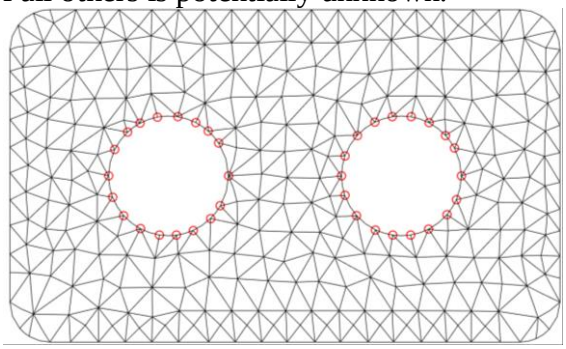

Figure 4 : Surface definition

As introduced in [2] defining a contact surface or a contact stiffness leads to nearly identical evolution of frequencies with the ability to compute the second evolution at a much lower numerical cost. It is thus proposed to model junctions using perfect contact in the minimal surface area and an out-of-plane (contact) $\nu$ and in-plane (sliding) $\tau$ stiffness values for the rest of the potential contact surface.

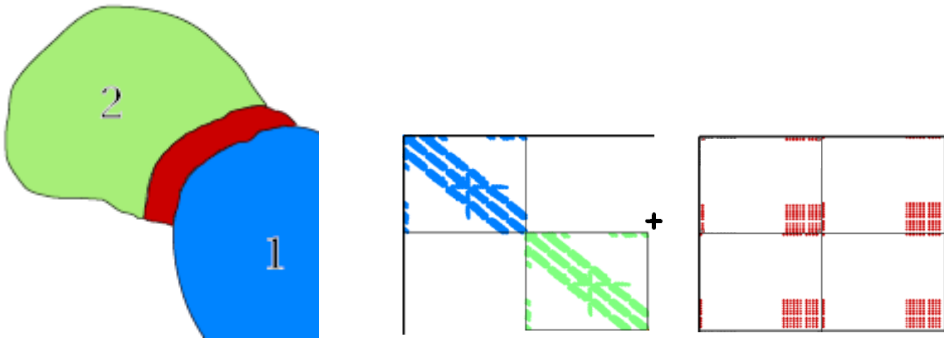


Figure 5 : FEM decomposition in component DOFs (blue and green) connected by a contact stiffness (red)

To integrate such a model in numerical computations, the system is decoupled in two components (see Figure 5), thus splitting the vector of Degrees of Freedom in two subvectors $q_1$ and $q_2$, and leading to equation of motion given by

$$[Ms^2 + K(\nu,\tau)]\begin{Bmatrix} q_1 \\ q_2 \end{Bmatrix} = \begin{Bmatrix} F_1(s) \\ F_1(s) \end{Bmatrix} \tag{1}$$

where, assuming that the junction mass is either null or can be neglected, the mass matrix topology is

$$[M] = \begin{bmatrix} M_1 & 0 \\ 0 & M_2 \end{bmatrix} \tag{2}$$

and the stiffness matrix can be decomposed into decoupled component stiffness, a fixed contact stiffness associated with the minimum contact surface, a normal stiffness proportional to coefficient $\nu$ and a tangential stiffness proportional to $\tau$

$$[K(\nu,\tau)] = \begin{bmatrix} K_1 & 0 \\ 0 & K_2 \end{bmatrix} + [K^J_{Fixed}] + \nu[K^J_N] + \tau[K^J_T] \tag{3}$$

Considering design points where $\nu = \tau$ the evolution of mode frequencies is shown in Figure 6. It clearly appears that a number of mode crossings could occur for a realistic range of junctions. The general objective of this study is to provide stiffness parameter candidates that lead to the best correlation, thus updating the assembly model, and to analyze in detail the influence of these mode crossings thus providing a design tool.

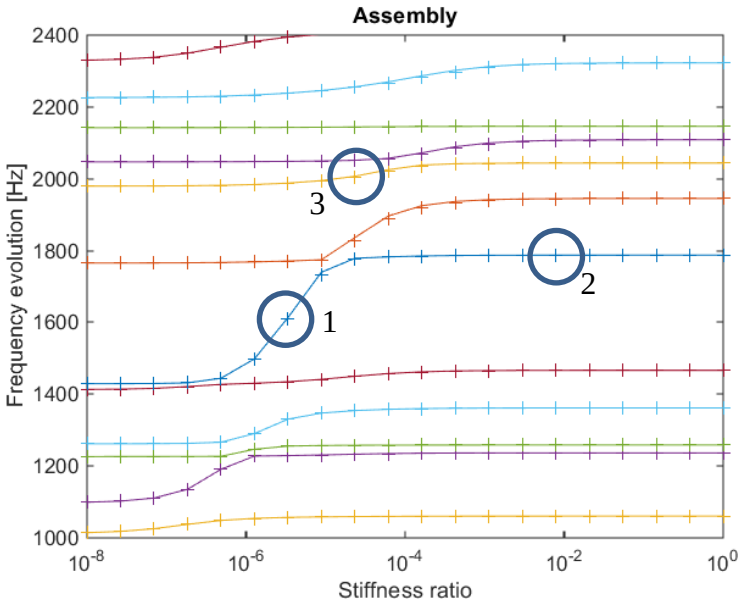


Figure 6 : Superposition of the mode frequency evolution with stiffness for the reduced model (lines) and the full model (crosses). O marks specific modes shown in Figure 8.

A major interest of contact definition with stiffness evolution is the ability to use multi-model reduction [1] for very fast computations. The full model is only computed at four operating points, which correspond to the extreme values of the two stiffness parameters and the associated collection of vectors is orthonormalized with respect to the mass $[M]$ and the stiffness matrix $[K(\nu_{MAX}, \tau_{MAX})]$ to generate a reduction basis

$$T_{Assembly} = [T(\nu_{MAX}, \tau_{MAX}), T(\nu_{MIN}, \tau_{MAX}), T(\nu_{MAX}, \tau_{MIN}), T(\nu_{MIN}, \tau_{MIN})]_{Orth} \quad (4)$$

of the subspace in which modes are computed. The reduction comes from the reduction of (1) into

$$([M_R]s^2 + [K_R(\nu, \tau)])\{q'\} = \left[\mathrm{T}_{\mathrm{Assembly}}\right]^T \begin{Bmatrix} F_1(s) \\ F_1(s) \end{Bmatrix} \quad (5)$$

with $[M_R] = \left[\mathrm{T}_{\mathrm{Assembly}}\right]^T [M] \left[\mathrm{T}_{\mathrm{Assembly}}\right]$ and $[K_R(\nu, \tau)] = \left[\mathrm{T}_{\mathrm{Assembly}}\right]^T K(\nu, \tau) \left[\mathrm{T}_{\mathrm{Assembly}}\right]$

The full and the reduced multi-models were computed for all operating points and show the errors to be very small, thus implying that the reduction space is sufficient to properly describe the evolution between the exactly resolved operating points. Figure 6 shows the almost exact superposition of mode frequencies computed with the reduced model (lines) and the full model (crosses). The gain of using a reduced model is both in terms of time (cost of 4 computations for hundreds of points in the design space) and memory (storing the reduced modeshapes associated with all points is practical when storing their full version would requires gigabytes).

The first obvious use of this parametric model is updating. One way to define the best global correlation can be the minimum of relative frequency shifts between paired modes. The objective function

$$J(\nu,\tau) = \sum_{j,k\ \text{pairs}} \left| \frac{f_j(\nu,\tau) - f_k(\nu,\tau)}{f_k(\nu,\tau)} \right| \quad (6)$$

can be displayed as a map (see Figure 7 left) where optimal couple is found at $\nu = 5e^{-7}$ and $\tau = 1e^{-4}$. On the right of the figure, the MAC is clearly improved. Some mode crossings corresponding to very close modes of the plate remain, but they span the same subspace so that the correlation result is satisfying.

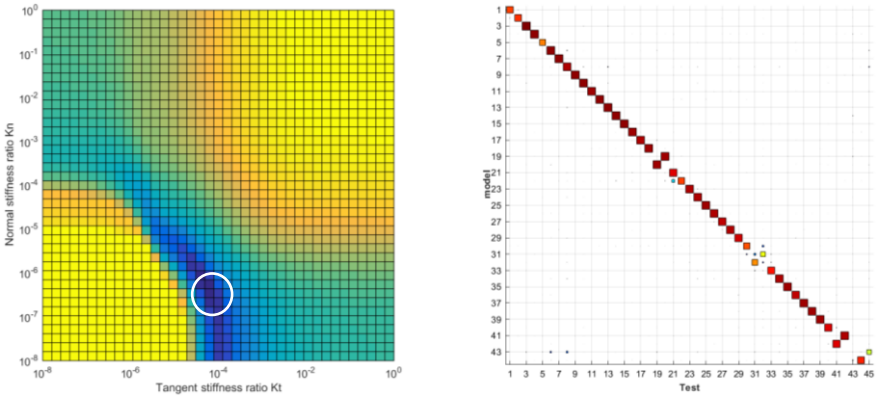


Figure 7 : Contact stiffness updating. Left : objective function in frequencies. Right: final MAC values.

## 3. UNDERSTANDING MODAL COUPLING

Looking now at the frequency evolution, some mode frequencies remain almost constant whereas others are very affected by the increasing of stiffness. Figure 8 shows three modeshapes. The first one corresponds to a rapidly increasing frequency. This modeshape is clearly dominated by bending of the cable guide. The second modeshape is in an area with very minor frequency evolution with stiffness increase. The deformation is only located in the plate and the cable guide is mostly following with rigid body displacement and no deformation. Finally, an intermediate case is shown where both the plate and the cable guide are deforming, which correspond to the coupling between the first bending mode of the cable guide and a plate mode.

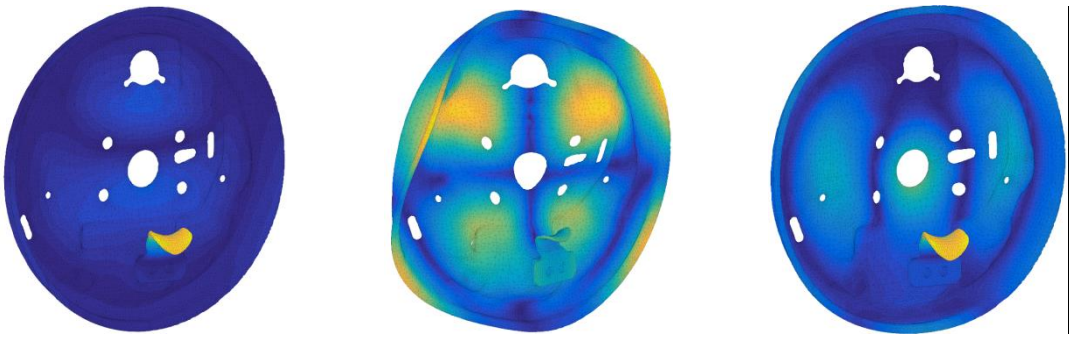

Figure 8 : Three modeshapes visualization corresponding to modes number 1, 2 and 3 showed in Figure 6

This highlights that with the stiffness increasing, the first bending mode of the cable guide is crossing plate modes and is coupled with them to a certain extent. When far from the plate modes, the cable guide bending mode is expressing alone with little deformation of the plate. In the same way, when far from the cable guide first bending mode, the plate modes are expressing alone with little contribution from the cable guide.

It is however obvious that the meaningful component mode depends from the presence of the other components. Here, the cable guide bending would be very different in free/free conditions. To gain a good understanding of the component mode integrated in the system, it is thus proposed to assume that the other component is “rigid”. This could be computed using

an arbitrarily high Young modulus, but that tends to lead to convergence problems. It is thus proposed here to restrict the displacements to rigid body modes, thus only keeping inertia effects of the constrained component. One thus seeks solutions within the subspace

$$\{q\} = \begin{bmatrix} RB_1 & & 0 \\ & \ddots & \\ 0 & & I \\ & & & \ddots \end{bmatrix} \{q'\} \tag{7}$$

As before, multi-model reduction is used to obtain frequency evolutions with stiffness shown in Figure 9. On the left, the plate is forced to be rigid and the only mode is the first cable guide bending whose frequency strongly depends on the contact stiffness varying in the 1200 to 2200 Hz range. The junction thus has a major effect on the cable guide component. On the right, the cable guide is rigid and only the plate modes for a rigid cable guide are shown. The junction impact is mild, so that the origin of variations is actually the changes in coupling with the cable guide mode. Understanding how shapes evolve throughout this parametric study is thus critical.

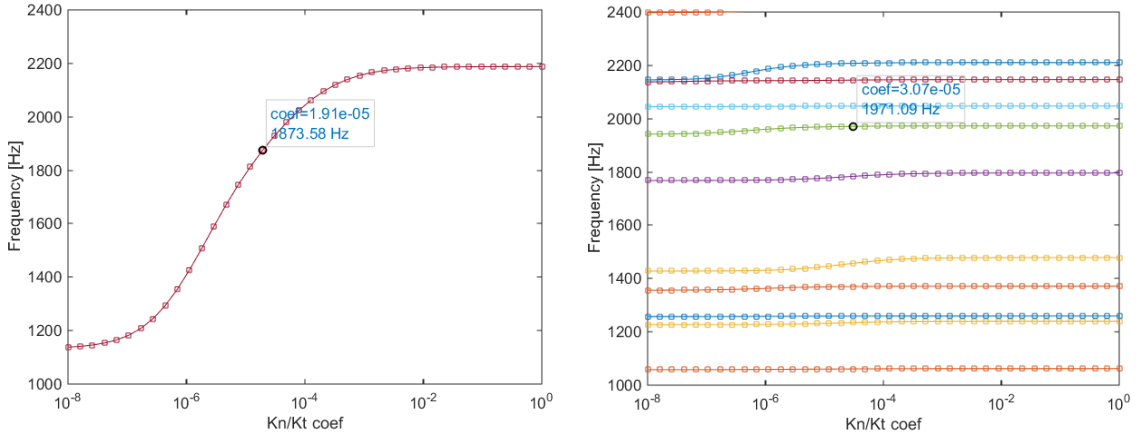


Figure 9 : Result of Assembly modes with RB comp evolution (plate RB / CG RB)

As the objective is to see which component mode contributes to an assembly mode, a definition of component mode amplitudes is introduced as follows. For each operating point $(\nu, \tau)$, the computed modeshapes satisfy the orthogonality condition

$$[\phi(\nu,\tau)^T][M][\phi(\nu,\tau)] = I \tag{8}$$

and an arbitrary shape can be decomposed on the modeshape basis

$$\{q\} = [\phi(\nu,\tau)]\{\alpha(\nu,\tau)\} \tag{9}$$

From (8), we can derive

$$[\phi(\nu,\tau)]^{-1} = [\phi(\nu,\tau)^T][M] \tag{10}$$

And thus, combining (9) and (10)

$$\{\alpha(\nu,\tau)\} = [\phi(\nu,\tau)^T][M]\{q\} \tag{11}$$

The modal amplitude of a given shape can thus be retrieved directly with the observer $[\phi(\nu,\tau)^T][M]$.

Assembly modes with rigid components can now be observed on the assembly modes to gain understanding of where they are playing a role. Figure 10 shows the participation of the first assembly mode with rigid plate on the assembly modes (strong dots mean high participation). As expected, it crosses many plate modes. It is sometimes coupled with them for large ranges of stiffness values and sometimes not coupled at all.

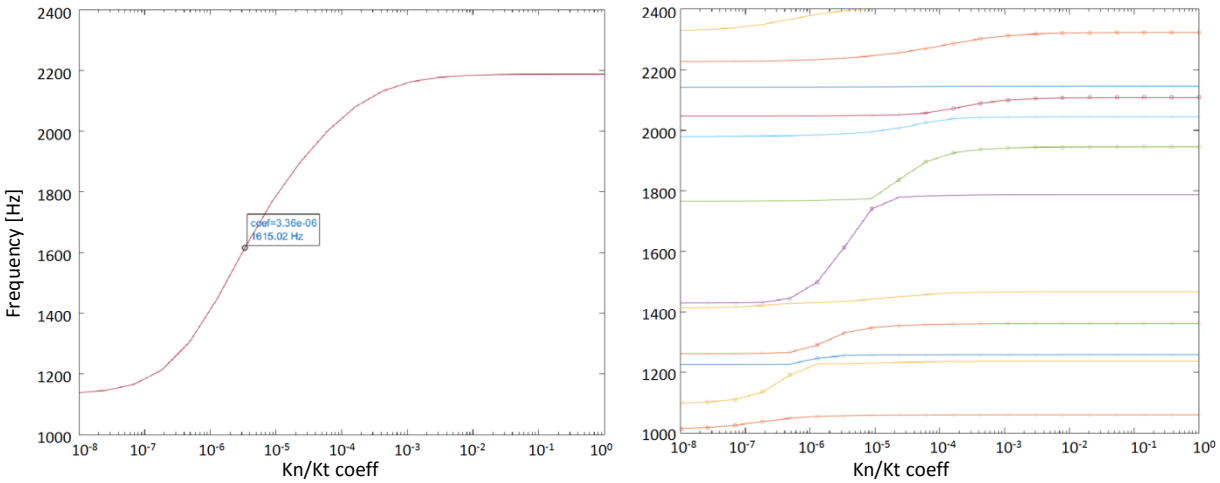


Figure 10 : Observation of the first assembly mode with rigid plate on the assembly modes.

Figure 11 shows the participation of one assembly mode with rigid cable guide (pointed on the left). One very interesting result is found here. Adding stiffness when a single component can deform (left of Figure 10 and Figure 11) increases the mode frequencies as expected. Considering the assembly mode with rigid cable guide selected on the left of Figure 11, its observation on the assembly mode (on the right of Figure 11) shows that at low stiffness values, this deformation of the plate is of higher frequency than at high stiffness value. This is due to the mode crossing by the first bending mode of the cable guide.

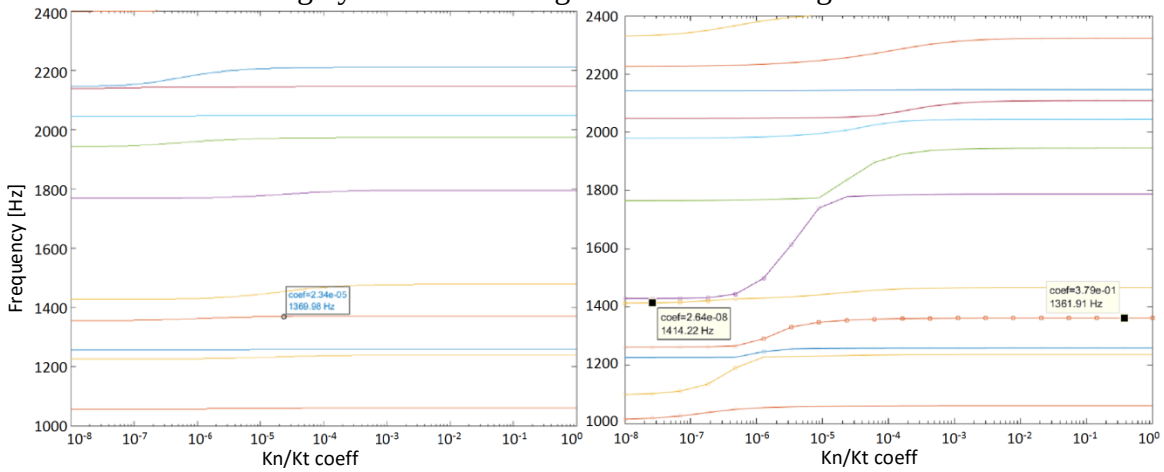


Figure 11 : Observation of an assembly mode with rigid cable guide on the assembly modes.

Figure 12 shows the two modeshapes selected on the right of Figure 11. At low stiffness, the modeshape frequency is higher than the cable guide bending mode frequency: they are in opposition of phase so that the frequency of the plate modeshape is higher. In the opposite, at high stiffness, the cable guide is following the deformation of the plate in-phase, thus adding mass and reducing the frequency.

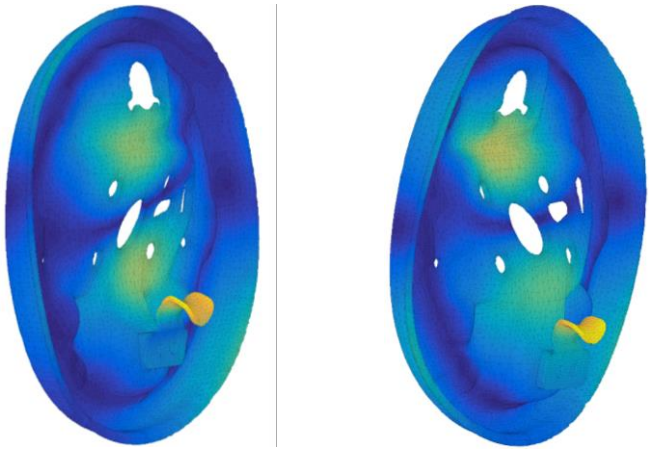

Figure 12 : Same plate shape deformation with higher frequency at low stiffness (left) and lower frequency at high stiffness (right)

## 4. SENSITIVITY ANALYSIS : IMPACT OF MODE CROSSING ON THE FRFs

The previous section focused on modal frequencies and shapes. But for the final application to squeal studies, the noise is actually analyzed through transfers where modal contributions are combined and each mode has a contribution associated with its controllability by the non-linear contact/friction forces. In practical cases which involve multiple modes, using transfers is thus more appropriate and will be the object of this section.

Figure 13 illustrates the evolution of a collocated transfer function for a point of the cable guide. The traditional Bode representation on the left illustrates shifts of frequencies and the presence of low amplitude points. But it is hard to interpret. The same plot viewed as an amplitude map in the frequency contact stiffness plane with modal frequencies shown as black lines, more clearly indicates that the cable guide contribution can switch within the 1000-2000 kHz band and depending on how it is coupled with plate modes the amplitude can go down significantly. Operating near areas of transition can be both interesting from the point of view of performance and dangerous from the point of view of robustness since relatively minor changes in junction properties may lead to large amplitude variations in the response.

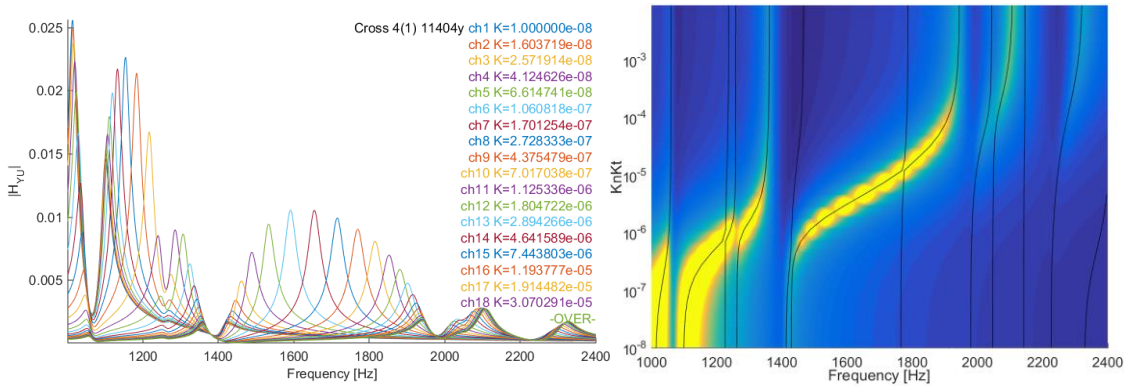


Figure 13 : Evolution of collocated transfer on the cable guide with contact stiffness (left). Viewing of the same data as a frequency joint stiffness map coding amplitude as color (right).

Figure 14 provides a second illustration where the plate mode near 2 kHz is excited for the chosen impact point. The transition clearly indicates that for a range of junction properties, coupling with the cable guide mode actually notably decreases vibration levels. In this case, the cable guide bending mode actually behaves as the well-known “proof mass damper”.

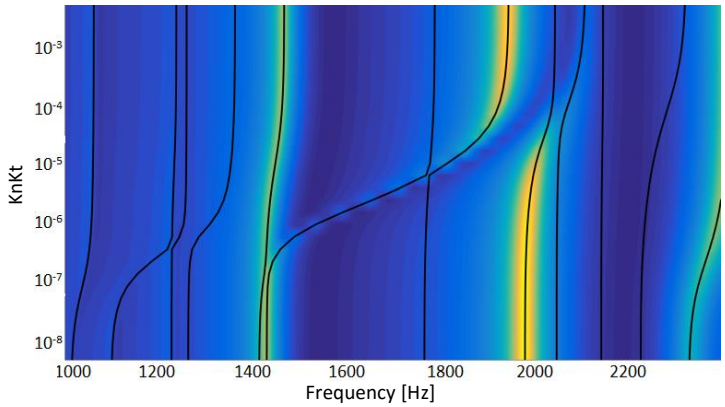


Figure 14 : Evolution with contact stiffness of collocated transfer on the plate

## CONCLUSION

The proposed application clearly illustrated the major impact of junctions on modal properties of assemblies. Efficient numerical strategies were introduced to allow interactive visualization of the design space. The evolution of modal frequencies and transfer functions was then analyzed in terms of coupling of component modes with the notion of component mode with within a rigid assembly appearing as quite relevant. These tools, if properly integrated within a design process combining test and updated FEM models, will provide a favorable environment to analyze squeal occurrences and the impact that junction or component modifications might have.

## REFERENCES

[1] C. Hammami, “Intégration de modèles de jonctions dissipatives dans la conception vibratoire de structures amorties,” Paris, ENSAM, 2014.
[2] G. MARTIN, E. BALMES, and T. CHANCELIER, “Review of model updating processes used for brake components,” presented at the Eurobrake 2015.
[3] R. J. Allemang, “The modal assurance criterion–twenty years of use and abuse,” *Sound Vib.*, vol. 37, no. 8, pp. 14–23, 2003.